

# A new method of estimating the ratio between in situ rock stresses and tectonics based on empirical and probabilistic analyses

L.I. González de Vallejo\*, T. Hijazo

Department of Geodynamics, Geological Engineering, Universidad Complutense de Madrid, 28040 Madrid, Spain

---

## A B S T R A C T

This paper describes a new procedure for assessing the ratio between in situ stresses in rock masses by means of  $K$  ( $K = \sigma_H / \sigma_v$ , being  $\sigma_H$  and  $\sigma_v$  principal stress) and tectonics for purposes of engineering geology and rock mechanics. The method combines the use of the logic decision tree and the empirical relationship between the Tectonic Stress Index, TSI, and a series of  $K$  in situ values obtained from an extensive database. The decision tree considers geological and geophysical factors affecting stress magnitudes both on the regional and local scale. The TSI index is defined by geological and geomechanical parameters. The method proposed provides an assessment of the magnitude of horizontal stresses of tectonic origin. Results for several regions of Europe are presented and the possible applications of the procedure are discussed.

### Keywords:

In situ stress  
Tectonic stress  
Geomechanical index  
Decision tree  
Logic tree  
Probabilistic methods

---

## 1. Introduction

In rock mechanics and engineering geology, certain properties of rock masses are generally estimated through empirical relationships. However, for in situ stresses, the available empirical relationships do not allow to estimate stress magnitudes within an acceptable range. In this paper  $K$  is defined as the ratio between the major horizontal stress ( $\sigma_H$ ) and the vertical stress ( $\sigma_v$ ) (Goodman, 1989), being  $\sigma_v$  the weight of overburden. Fig. 1 shows  $K$ -depth relationships using the stress data compiled in this study. Envelope lines obtained from these data and those proposed by Hoek and Brown (1980) are also included in Fig. 1. Large variation in the value of sigma H at the depths commonly dealt with in engineering is observed. Other methods of estimating stresses (Sheorey, 1994) are based on the thermoelastic properties of rocks, but do not consider the main factors affecting the state of stress of the rock. Approaches such as geological (tectonic structure analysis), seismic (focal mechanisms) give an estimate of the orientations of stresses but not their magnitude. Indirect estimation methods include acoustic emission (AE), anelastic strain recovery (ASR) measurements (Villaescusa et al., 2002; Lin et al., 2003) and borehole breakouts and core diskings. Available procedures to directly

measure stress magnitudes such as hydrofracturing, overcoring, or doorstopper techniques are described by ISRM (2003).

In this paper, a new procedure is described whereby the value of  $K$  ( $\sigma_H / \sigma_v$ ) can be estimated for a given rock mass. The method is based on applying the probabilistic decision tree method and the empirical relationship between the TSI (Tectonic Stress Index) and  $K$ . The decision tree considers the geodynamic and geophysical factors that determine horizontal stress magnitudes on both a regional and local scale and results are expressed qualitatively as very high, high, intermediate or low magnitudes along with the possibility of local stress amplification effects. The TSI takes into account the geological history of the rock, its elastic modulus and the maximum lithostatic load. Using a large world database of in situ measurements of  $K$ , empirical correlations between  $K$  and TSI have been established. The results of applying these correlations to a wide range of cases are presented.

## 2. Factors affecting the state of stress

Any method of evaluating the state of stress for rock mechanics and engineering geology purposes needs to consider the factors affecting natural stresses, including the origins and the mechanisms that generate these stresses, as well as their spatial distribution and magnitude. Table 1 provides a summary of the main models and hypotheses proposed to explain the origins and formation mechanisms of the stresses affecting the Earth's crust or upper elastic lithosphere.

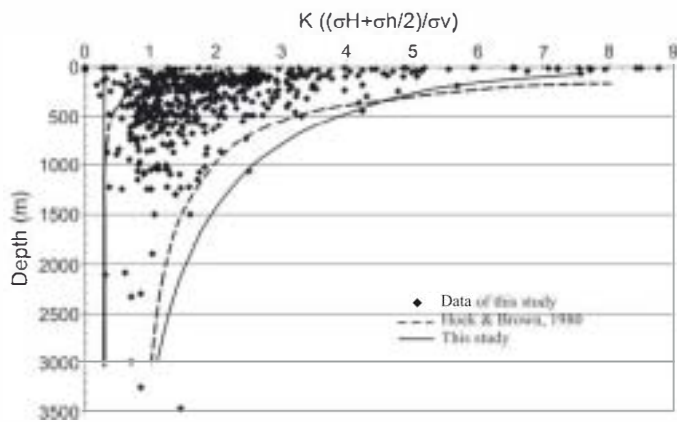


**Fig. 1.** Variations in  $K$  with depth based on world data compiled for this study. — Present study, - - - Hoek and Brown (1980). For the purpose of comparing the envelopes lines used by Hoek and Brown and the stress database used in this paper.  $K$  values have been plotted as defined by Hoek and Brown:  $K = (\sigma_H + \sigma_h / 2) / \sigma_v$ .

Tectonic stresses are the main causes of stress in the lithosphere and are generated through two basic mechanisms (Fig. 2):

Plate boundary forces generated by the movement of tectonic plates give rise to compressive or extension stresses. These stresses can reach magnitudes of 50 MPa at collision borders and 20 MPa at expansion margins (Park, 1988).

Forces produced by isostatically compensated loads due to large topographical elevations (mountain ranges) whose weight is compensated by zones of less lithospheric density or by an increase or reduction in crust thickness. This mechanism of isostatic compensation leads to a combined effect of vertical loads and a rising push (buoyancy forces), generating horizontal stresses in adjacent zones. Their magnitudes can be of the order of 50 MPa (Park, 1988).

Both types of stress are permanent and continuous over geological time and constitute the so-called renewable stresses. Coexisting with these stresses are those denoted non-renewable. These are not tectonically significant since they are not long-standing, being gradually released over time. However, they do give rise to brittle fractures and creep processes. The main non-renewable stresses are (Bott and Kuszniir, 1984):

- Flexural stresses, due to non-isostatically-compensated loads.
- Membrane stresses, due to changes in the Earth's curvature.
- Thermal stresses, due to differential heat gradients.

Loading stresses, due to sedimentary processes, piling volcanic rocks, glacial ice deposition or unloading stresses due to erosion and ice retreat.

The regional distribution of stresses depends on the prevailing tectonic regime. Two large types of setting can be distinguished:

Intraplate regions in which compressive stresses predominate, which are largely uniform both in terms of their orientation and geographical extension. In these intraplate zones, the orientation of the compressive stress field depends of on the following factors: compressive plate margin forces, ridge push and continental collision stresses as well as the geometry of the plate margins on which they act. Discrepancies both in magnitudes and orientations can be attributed to buoyancy forces (Zoback et al., 1989).

Continental regions with large mountain systems. Here, the predominance of extensive stresses affects the different tectonic settings (continental collision, intraplate rift, back-arc regions). In some cases, changes in the direction of extension stresses are related to lateral changes in the thickness of the lithosphere and heat flow differences.

The distributions and orientations of stresses on continental and regional scales can be found in the World Stress Map (WSM) (Zoback et al., 1989; Reinecker et al., 2004).

The factors that most affect stress magnitudes are:

Rheological behaviour. On the lithospheric scale, this behaviour controls the relationship between stress magnitude and depth, and depends on the heat gradient and on crust composition and thickness.

Heat flow affects stress magnitudes, such that the greater the heat flow, the greater is the amplifying effect of stresses in the most superficial zone of the lithosphere, in which brittle behaviour predominates. Conversely, in the lower part in which the predominating behaviour is ductile, stresses decrease with depth (Kuszniir, 1991). The concept of amplifying effect of stresses due to build-up of stresses in the upper most elastic part of the lithosphere. This effect is the consequence of the more ductile behaviour of the lower lithosphere compared to the upper lithosphere, which leads to transfer of stresses from the lower to upper area (Kuszniir and Bott, 1977). The effect is most intense in plate margin zones.

Crust thickness. Since the upper crust layer is mainly comprised of quartz and feldspar and the lower layer of olivine, the uppermost portion of the crust is weaker. Thus for high crust thicknesses, the proportions of quartz and feldspar will exceed that of olivine and stress magnitudes will be lower.

Rock composition and its geomechanical behaviour. These two factors are linked: depending on the nature of the rock, its geomechanical behaviour will be more brittle or ductile, thus affecting strength and state of stress.

The area affected by plate margin forces depends on the thickness of the elastic crust enduring these forces. Thus, the greater the thickness the higher the wavelength or surface affected by the applied forces.

Time of stress. As the time of stress increases, so does the amplification effect along with the thickness of the elastic crust. However, due to this increased thickness, stress magnitudes are lower in intraplate and low heat flow regions (cratons), than in more tectonically active regions with high heat flows and a thinner crust (Kuszniir and Bott, 1977). In regions in which moderate or low stresses are exposed to a prolonged period of tectonic forces, the effect may be comparable to that experienced by regions of high or

**Table 1**  
Stress models

Bott and Kuszniir (1984)	
Renewable stresses (subjected to amplification)	Plate margin forces Forces due to isostatically-compensated loads
Non-renewable stresses (not subjected to amplification effects)	Flexural stresses Membrane stresses Thermal stresses
Zoback et al. (1989)	
First category stresses	Plate margin forces Forces generated by geodynamic processes Thermoelastic forces Shear forces at the base of the lithosphere Forces arising from plate geometry
Second category stresses	Flexural stresses Buoyancy forces

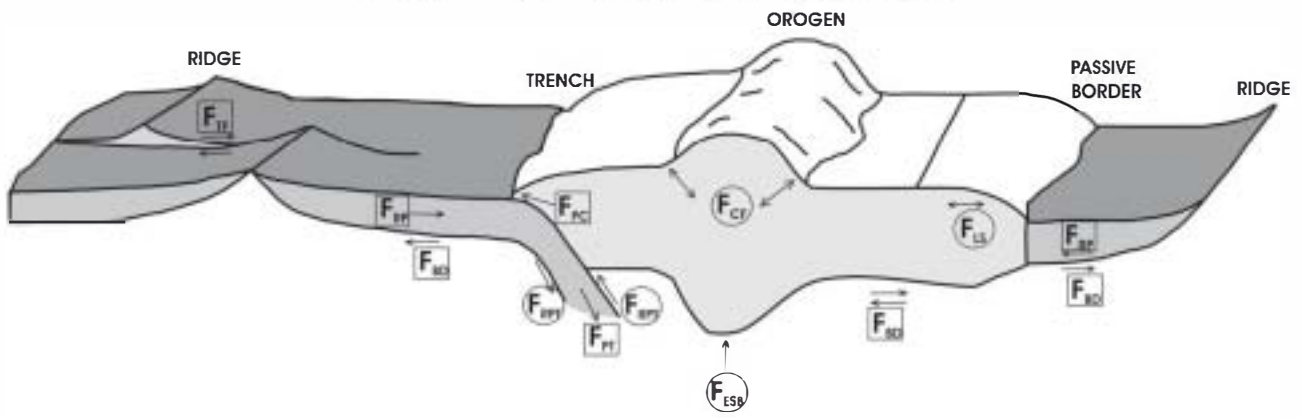


**Fig. 2.** Locations and relative orientations of forces generating stress fields in the lithosphere:  $F_{TF}$  (plate traction);  $F_{RP}$  (ridge push);  $F_{RT}$  (resistant to the plate);  $F_{CP}$  (plate contact);  $F_{TF}$  (transformant faults);  $F_{BD}$  (basal drag);  $F_{ESB}$  (extensive stress linked to lateral density variations and buoyancy forces);  $F_{CR}$  (crust flexion);  $F_{LS}$  (lateral strength differences), modified from [Olaiz et al. \(2006\)](#).

very high stresses sustained over a shorter time period ([Zoback et al., 1989](#)).

**Residual stress.** Can remain in rock masses which have been subject in the past to higher stresses than they are subject to today to different conditions, so that allow the rock to reach a new internal equilibrium under reduced load or temperature changes. These stresses were found to be relatively small compared to the high horizontal stresses measured at shallow depth ([Amadei and Stephansson, 1997](#)).

In summary, the factors that mostly affect the magnitude of natural stresses are: crust thickness, heat flow, time over which stresses are sustained, and the composition and heterogeneities of the crust. To a similar extent as crust thickness, the predominant factor is heat flow and therefore the value of  $\sigma_H$  is greater in regions of high heat flow. In contrast, like the heat flow, crust thickness controls magnitude such that lower  $\sigma_H$  values are observed for great thicknesses, as it has been previously explained.

Local factors can also substantially modify both the magnitude and orientation of stresses. These include: rock composition, faults or fractures, sedimentary loads, topographic effects and glacial unloading.

[Fig. 1](#) illustrates how stress magnitudes change with depth, and shows the variation in  $K$  with depth for the data set recompiled for the present study. The figure indicates the lower and upper limits of  $K$  according to depth as reported by [Hoek and Brown \(1980\)](#), which may be compared with the present limits. In both cases, the value of  $K$  is clearly greater than 1 and may even exceed 6 for the first 500 m of depth, dropping to 2 beyond depths of 1000 m and tending towards values close to 1 at depths of 2000 to 3000 m, despite few  $K$  measurements available for these depths.

### 3. Use of the decision tree to estimate horizontal stress magnitudes

The decision tree procedure is based on the logic tree method that is widely used in engineering and well known in seismic hazard analysis ([Coppersmith and Young, 1986](#); [EPRI, 1987](#); [Reiter, 1990](#); [US Army Corps of Engineers Internet Publishing Group, 1999](#)). It is a tool for helping to choose between several course of action. It provides a highly effective structure within which it can be laid out options and investigate the possible outcomes of choosing those options. The decision tree estimates the likelihood that the particular question addressed will be true. Its results represent a degree of confidence in the prediction rather than a probability ([Bommer et al., 2005](#)). The

expert evaluates the magnitude of major horizontal stress as a function of the different factors considered in the tree that contribute to the state of stress. Hence, certain criteria need to first be established ([Table 2](#)) to qualitatively assess these magnitudes (as high, intermediate or low).

Like a logic tree, a decision tree is comprised of nodes and branches. Each node represents a variable or state of the process to be analysed. Each branch indicates a possible option and is assigned a probability value or degree of confidence that the node or variable is correct. All branches lead to nodes that are true states, and their probability value depends on the degree of confidence or knowledge of the question considered. Once these probability values have been assigned to each branch, all the probabilities of the different branches arising from the same node should add up to 1. The final node is assigned a percentage or degree of confidence based on the relative influence of the different contributing factors.

To use this method to estimate horizontal stress magnitudes, the main factors affecting the state of stress described in [Section 2](#) were included. To this end, two decision trees were constructed. The first (tree 1, [Fig. 3](#)) included regional factors affecting horizontal stresses. Its results indicate whether stresses are low, intermediate or high. For the present purposes, stresses were defined as low if their magnitude was less than 10 MPa, intermediate if it was 10 to 25 MPa, high if 25 to

**Table 2**

Factors contributing to the state of stress considered in the decision tree to estimate horizontal stresses

Factors	Magnitude of predicted horizontal stresses		
	High	Intermediate	Low
Geodynamic setting		Intraplate (non-cratonized regions)	Intraplate (cratons)
	Convergent plate margin	Convergent plate margin and transforming fault	Divergent plate margin
Heat flow	High	Intermediate	Low
Crust thickness	Low	Intermediate	High
Geomechanical behaviour	Fragile, high strength and elastic	Fragile, moderate strength, resistant and elastic	Ductile, low strength and low elasticity
Tectonic structures	Compressive	Compressive and strike-slip	Extensive
Topographic effect	Very high relief or abrupt relief	High to moderate relief	No topographic effect
Preexisting overloads	High erosion	Moderate erosion	No appreciable effect
Tectonized zones	Very tectonized	Predominant fractures	Absence of or few fractures

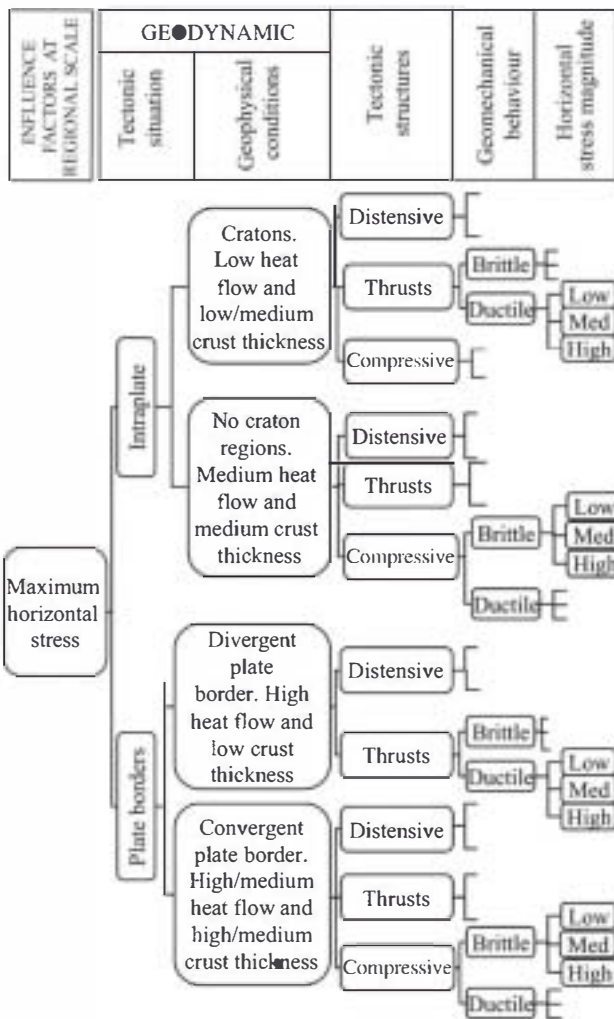


Fig. 3. Decision tree 1: estimating the magnitudes of horizontal stresses due to regional contributing factors.

40 MPa and very high if greater than 40 MPa; always for depths of less than 2000 m. In the second tree (tree 2, Fig. 4), local factors were considered, that is, factors that could amplify horizontal stresses through local effects. The degree of confidence adopted for this analysis was at least 60%.

The following factors were considered for tree 1:

**Geodynamic setting:** intraplate or plate margin regions. For the purpose of this study, a plate margin region was defined as one whose deformation is directly associated with the actions of the plate margin. Examples of this type of deformation are the large orogens of the Alps, Andes, Himalayas or areas close to a rift or dorsal.

**Crust thickness:** the following intervals were established:

High crust thickness:  $\geq 30$  km (orogen and cratons).

Intermediate crust thickness: 15 to 30 km (intraplate regions).

Low crust thickness:  $< 15$  km (generally the ocean crust).

**Heat flow:** the ranges established were:

High heat flow:  $\geq 80 \text{ mW m}^{-2}$  (regions close to a plate margin).

Intermediate heat flow: 45 to  $80 \text{ mW m}^{-2}$  (intraplate regions with recent tectonics).

Low heat flow:  $< 45 \text{ mW m}^{-2}$  (cratonized regions).

**Tectonic structures.** The structures considered here were of the compressive type: folds, inverse fractures and overthrusts. Extensional structures were taken to be normal faults.

Geomechanical behaviour. This factor was considered at the regional scale according to the brittle or ductile behaviour of the materials. If the materials are brittle, the tectonic setting will be characterized by fractures or normal or inverse faults; in ductile materials, the tectonic environment will be characterized by folds, which are common in sedimentary settings.

For tree 2, the following factors were considered:

**Topographical effects:** these occur in regions with large elevations and deep valleys. In areas of marked relief the orientations and magnitudes of the main stresses are modified.

**Preexisting overloads:** loads of sediments or of layers of ice of glacial origin; erosion or ice retreat increase the relative value of horizontal stresses.

**Presence of faults and fractured zones:** if the region analysed occurs in an area tectonized by faults and other tectonic structures or is close to this region, horizontal stresses may be locally amplified.

Table 2 shows the factors included in the trees used to estimate the relative magnitudes of the horizontal stresses that might be expected.

#### 4. Estimation of $K$ from TSI

The TSI was defined according to the expression (González de Vallejo et al., 1988)<sup>1</sup>:

$$TSI = \log(T/(E \cdot H)) \cdot NC \cdot SC \quad (1)$$

where

$T$  age of the first orogenic cycle or main folding period affecting the rock mass (years)

$E$  elastic modulus of the rock matrix (GPa)

$H$  maximum lithostatic load supported throughout its geological history (metres)

$NC$  coefficient of seismotectonic activity

$SC$  coefficient of topographic influence.

The age ( $T$ ) of the main folding period or orogenic cycle is related to the time elapsed since the main deformation of the rock was produced. In effect, this time constitutes one of the factors contributing to the stress state as mentioned above in Section 2. For the TSI, it is assumed that the main orogenic period corresponds to peak tectonic stresses and that subsequent to this deformation, tectonic stresses diminish with time. In the TSI,  $T$  is referred here to the orogeny of the Hercynian (250–300 M.a.) and Alpine (10–12 M.a.), although we also considered the Caledonian orogeny (600 M.a.). In the situation of a single rock mass being affected by several orogenies, only the most ancient of these was considered.

The variable  $E$  is related to the petrophysical properties of the rocks along with processes of diagenesis, compacting, lithification, deformation and recrystallization. High values of  $E$  generally indicate highly resistant rocks able to sustain high stresses before they deform or break. Values of  $E$  lower than 25 GPa are not valid for applying the TSI. Notwithstanding, if the same rock mass showed several lithologies, the highest  $E$  value was considered.

The variable  $H$  indicates the maximum lithostatic load to which the rock has been subjected over its geological history. For sedimentary rocks,  $H$  is equivalent to the maximum thickness of sedimentary deposits within an error range lower than  $\pm 500$  m. A rough estimate of  $H$  can be made from the peak heights of the

<sup>1</sup> The expression defined in reference González de Vallejo, 1988 was:  $\log SRF = (T/(E \cdot H)) \cdot NC \cdot SC$  (SRF = stress relief factor). In this paper SRF has been substituted by TSI (tectonic stress index) which better describes this parameter.

sedimentary setting. Moreover, the tectonic structure in which the zone examined is emplaced should be taken into account, since in regions with overthrusts or inverted folds, part of the stratigraphic sequence may be repeated, increasing the value of  $H$ .

For igneous rocks,  $H$  corresponds to the depth at which the rocks were emplaced and acquired their elastic properties. This depth is estimated within a margin of error of less than  $\pm 1000$  m. For extrusive, or volcanic igneous rocks,  $H$  is determined as for sedimentary rocks, that is, calculating the current stratigraphic column taking into account possible eroded levels. For intrusive, or plutonic, rocks,  $H$  is estimated according to the emplacement depth of the intrusive body. This depth may be inferred from several criteria such as texture, grain size, contacts between the wallrock and intrusive rock; three emplacement depth levels being differentiated (Buddington, 1959):

**Epizone:** depth less than 8 km. A vast contrast between the temperature of the magma and surrounding wallrock gives rise to rapid crystallization and small grain sizes. The wallrock is usually affected by contact metamorphism. Contacts between the pluton and wallrock are angular and discordant, and the high temperature difference gives rise to porphyric and aplitic textures.

**Mesozone:** In the middle crust at depths of 8–12 km. Contacts are angular and discordant as well as gradational and concordant. Foliation in plutons is scarce and often chemically and mineralogically zoned. The metamorphic contact zone is extensive and the pluton shows flow structures.

**Catazone:** Emplaced at depths greater than 12 km. The temperature difference between the magma and wallrock is small and this gives rise to large crystal sizes. The wallrock rock is of high-grade metamorphism. Contacts between the pluton and wallrock are concordant and gradational. Plutons generally show a foliation pattern consistent with that of adjacent metamorphic rocks. Migmatites appear.

For metamorphic rocks,  $H$  can be estimated from the minerals comprising the rock as pressure and temperature indicators (geobarometers and geothermometers), and from these variables the depth

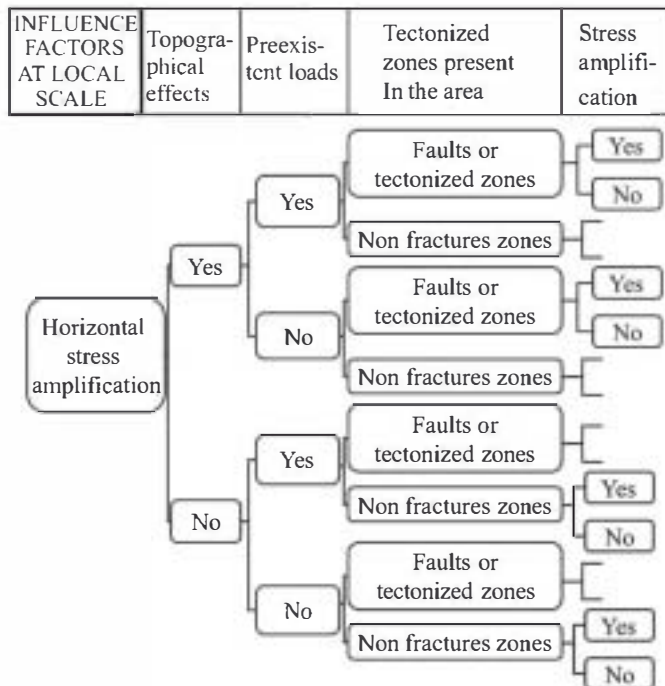


Fig. 4. Decision tree 2: estimating the likelihood of amplification effects on the magnitudes of horizontal stresses due to local contributing factors.

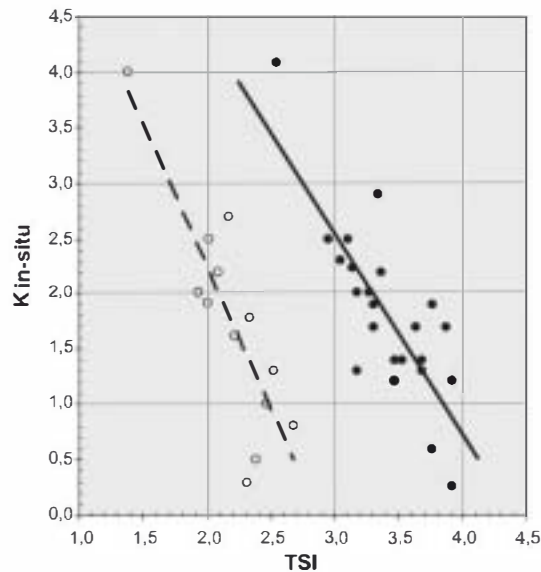


Fig. 5. Relationship between in situ determined  $K$  values and the TSI using the TSI88 database (González de Vallejo et al., 1988). ● Hercynian rocks; ● Alpine rocks; — global relationship for Hercynian rocks; — global relationship for Alpine rocks.

at which they formed can be estimated. As a simplification, three zones related to the degree of metamorphism can be distinguished:

**Low-grade metamorphism:** temperatures between 200 and 450 °C, depths between 5000 and 7000 m. The most common minerals are talc, epidote, chlorite and serpentine. Characteristic rocks: quartzites, slaty granites, milonitized granites, phylites and slates.

**Intermediate-grade metamorphism:** temperatures between 450 and 650 °C, depths between 7000 and 12000 m. The most common minerals are biotite, hornblende, staurolite and andalusite. Characteristic rocks: quartzites, micaceous slates, marbles, amphibolites and eclogites.

**High-grade metamorphism:** temperatures between 650 and fusion, depths between 12000 and 20000 m. The most common minerals are sillimanite, forsterite, wollastonite, garnierite, olivine and garnet. Characteristic rocks: orthogneisses, paragneisses, granulites, graphites and hornblende gneisses.

For the TSI, Eq. (1) includes the coefficients NC and SC. NC is the coefficient of seismotectonic activity and was fixed at 0.25 for zones close to seismogenic faults or to plate boundaries; its value is 1 in the absence of these conditions. The SC, or coefficient of topographic influence, was fixed at 0.3 for zones close to steep slopes or deep valleys, and at 1 when these conditions were not met. In cases where both NC and SC are applicable only the 0.25 value must be considered. These coefficients were estimated from the TSI88 database (González de Vallejo et al., 1988).

### 5. Relationships between $K$ and TSI

The first relationship between  $K$  and the TSI was derived from a database of 38 data denoted TSI88 (González de Vallejo et al., 1988) corresponding to 38 different zones in which several in situ stress measurements were taken to give a mean  $K$  value (Fig. 5). The instrumental  $K$  values are the mean values on each site. These relationships were:

For rocks deformed during the Hercynian orogeny:

$$K_{ssher} = -1.81 \cdot TSI + 7.96. \quad (2)$$

For rocks deformed during the Alpine orogeny:

$$K_{ssalp} = -2.57 \cdot TSI + 7.38. \quad (3)$$

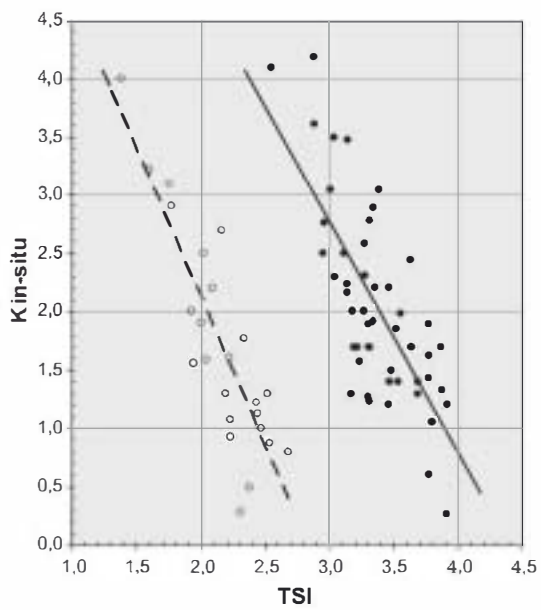


Fig. 6. Relationship between in situ-determined  $K$  values and the TSI using the TSI'04 database (Hijazo, 2004). ● Hercynian rocks; ● Alpine rocks; — global relationship for Hercynian rocks; — — global relationship for Alpine rocks.

From a subsequent database, TSI'04 (Hijazo, 2004) comprising 74 sites, we obtained the following  $K$ -TSI relationships (Fig. 6):

For rocks deformed during the Hercynian orogeny:

$$K_{04her} = -1.99 \cdot TSI + 8.73. \quad (4)$$

For rocks deformed during the Alpine orogeny:

$$K_{04alp} = -2.55 \cdot TSI + 7.23. \quad (5)$$

By incorporating new stress magnitude data, the TSI'06 database was compiled. 13 854 magnitude data from the World Stress Map

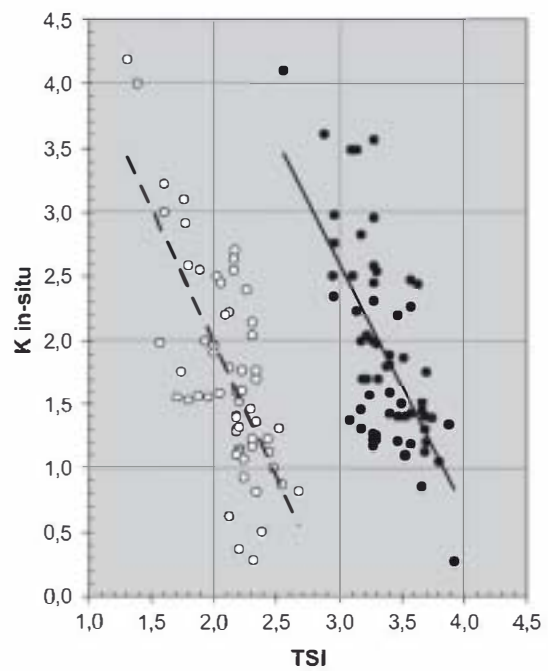


Fig. 8. Relationship between in situ-determined  $K$  values and the TSI using the TSI'06 database. ● Hercynian rocks; ● Alpine rocks; — global relationship for Hercynian rocks; — — global relationship for Alpine rocks.

(WSM), literature review and underground work projects have been analysed (Fig. 7). From these data, 172 were selected on the basis of their acceptable quality in terms of the techniques used for magnitude measurements and coherency in results, along with geological and geomechanical information on the rock mass. Each datum corresponds to a different site, the mean value of  $K$  being taken as representative of the given site.

The  $K$ -TSI relationships obtained from the TSI'06 database are provided in Fig. 8. The incorporation of WSM world data has meant a greater variation of data for the  $K$ -TSI relationship, owing both to local

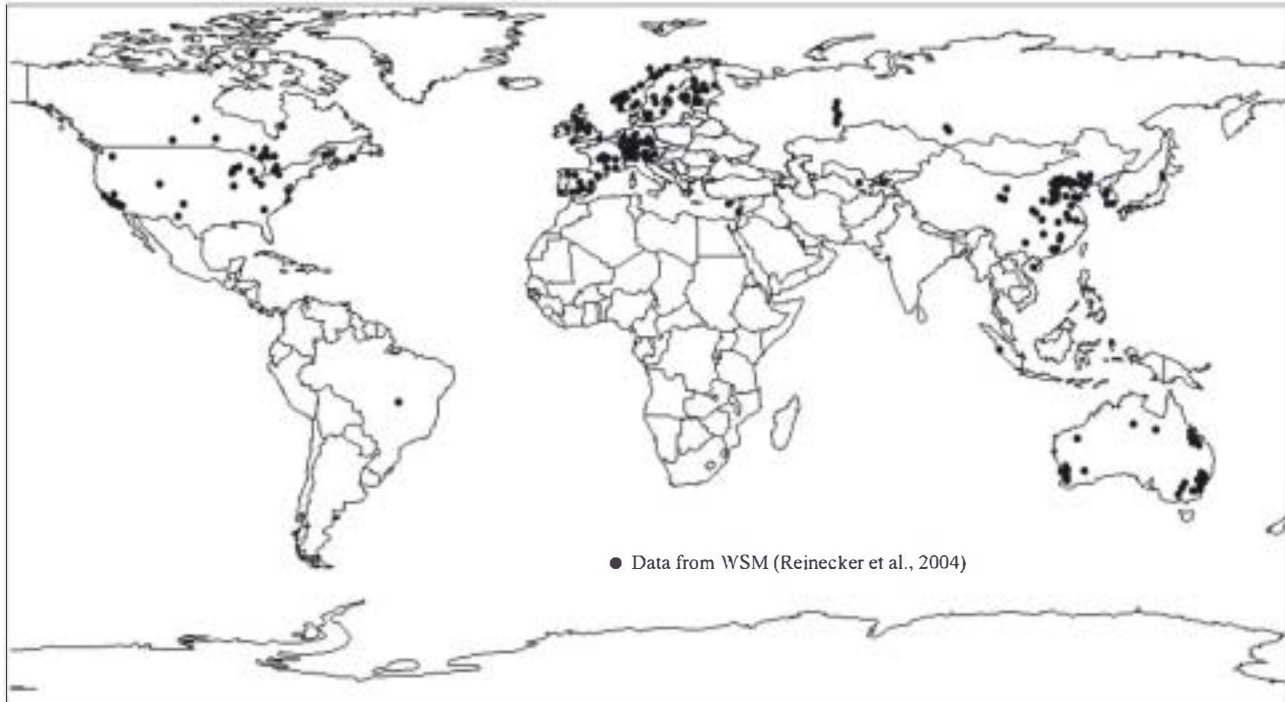


Fig. 7. Locations of stress magnitude measurements in the TSI'06 database.

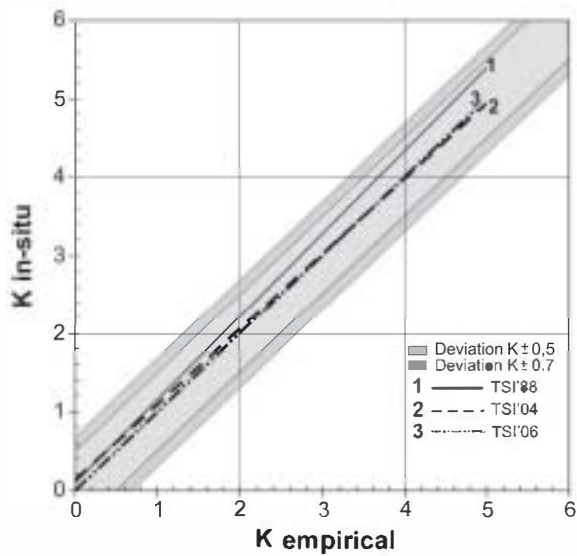


Fig. 9. Linear relationships generated by minimum-square fitting in situ  $K$  to empirical  $K$  using the data from Fig. 8 for Hercynian rocks.

anisotropies and to uncertainties in  $E$  and  $H$ , whose values were indirectly determined. The following  $K$ -TSI relationships were obtained:

For rocks deformed during the Hercynian orogeny:

$$K_{06her} = -1.93 \cdot TSI + 8.38. \quad (6)$$

For rocks deformed during the Alpine orogeny:

$$K_{06alp} = -2.09 \cdot TSI + 6.15. \quad (7)$$

When the three  $K$ -TSI relationships obtained from the three databases were compared,  $K$  values derived from the  $K$ -TSI'06 relationship were found to best fit the  $K$  values provided by in situ determinations, both for the Hercynian and Alpine rocks (Figs. 9 and 10). In other words, the in situ  $K$ -empirical  $K$  relationship for the '06 database was closest to the ideal relationship (in situ  $K$  = empirical

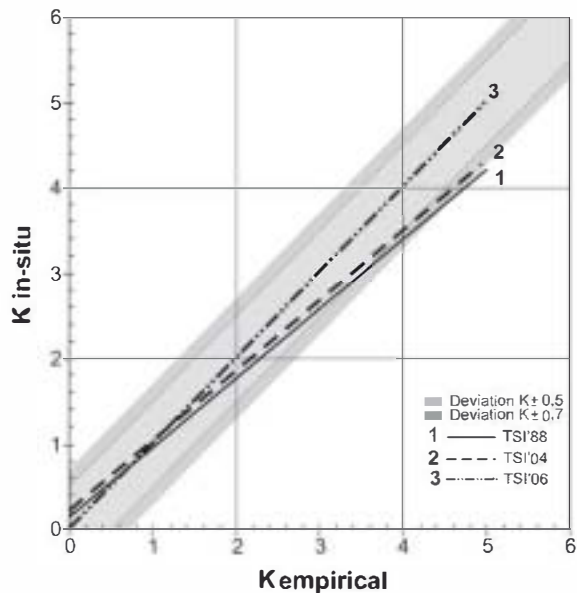


Fig. 10. Linear relationships generated by minimum-square fitting in situ  $K$  to empirical  $K$  using the data from Fig. 8 for Alpine rocks.

Table 3  
Ranges of  $K$  and possible tectonic stresses indicated by the TSI

Rocks folded in the Hercynian			Rocks folded in the Alpine		
TSI	$K_{06her}^a$	Stress <sup>b</sup>	TSI	$K_{06alp}^a$	Stress <sup>b</sup>
>3.80	<1.00	Low	>2.46	<1.00	Low
3.80-3.55	1.00-1.50	1.00-1.49	2.46-2.25	1.00-1.49	Medium
3.54-3.30	1.50-2.00	High	2.24-1.99	1.50-2.00	High
<3.30	>2.00	Very high	<1.99	>2.00	Very high

<sup>a</sup>  $K_{06}$  =  $K$  estimated from the TSI using the 2006 database.

<sup>b</sup> Stress indicates tectonic stresses.

$K$ ). In each case, the complete set of data such that the relationship obtained is the global scope has been used.

According to these results, several intervals of  $K$  and associated horizontal tectonic stresses as shown in Table 3 were established. As most of the database used to correlate  $K$  and TSI comes from hydrofracturing tests,  $\sigma_H$  and  $\sigma_v$  are considered as principal stresses. An estimation of  $\sigma_H$  can be obtained from  $K$  and  $\sigma_v$ .

## 6. Application to several regions of Europe

The method described was applied to several regions of Spain, Germany, France, Italy, Switzerland and Austria. In Spain, 25 zones for which we have in situ stress magnitude measurements were examined. Fig. 11 shows the  $K$ -TSI relationships obtained, indicating that most  $K$  values range from 1-2 and that the  $K$ -TSI relationship both for Hercynian and Alpine Spain is similar to the  $K$ -TSI relationship obtained for the entire data set (6) and (7). The  $K$ -TSI relationships for Spain are:

For rocks deformed during the Hercynian orogeny:

$$K_{Spainher} = -2.27 \cdot TSI + 9.51. \quad (8)$$

For rocks deformed during the Alpine orogeny:

$$K_{Spainalp} = -2.45 \cdot TSI + 7.27. \quad (9)$$

If we compare the  $K$  values determined in situ (in situ  $K$ ) with those obtained by the TSI (empirical  $K$ ) using Eqs. (6) and (7), 72% of

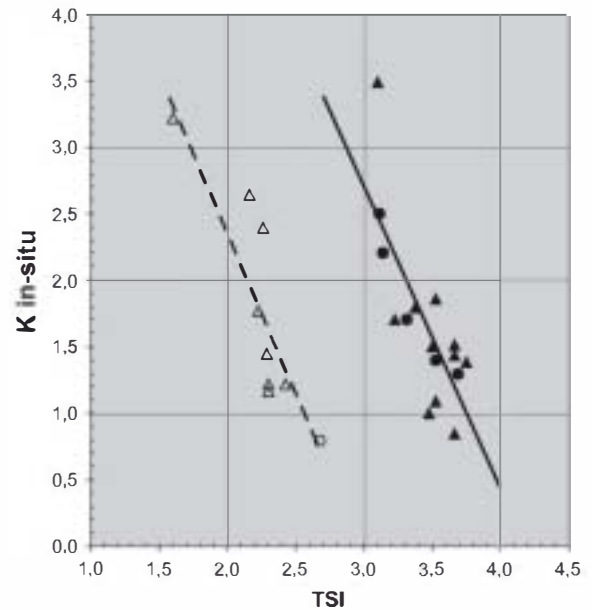


Fig. 11. Regional  $K$ -TSI relationships for Spain.  $\blacktriangle$  Hercynian rocks (hydrofracturing);  $\bullet$  Hercynian rocks (overcoring);  $\Delta$  Alpine rocks (hydrofracturing);  $\blacksquare$  Alpine rocks (overcoring); - - regional  $K$ -TSI relationship for Spanish Hercynian rocks; — regional  $K$ -TSI relationship for Spanish Alpine rocks.

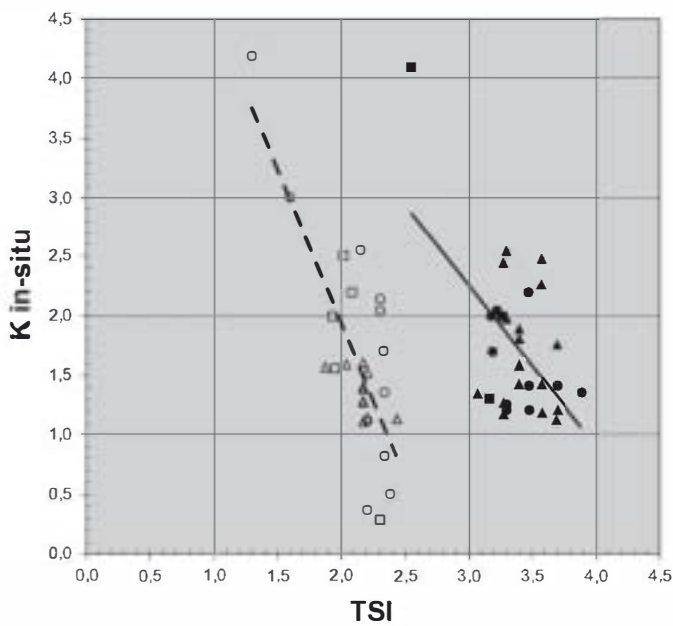


Fig. 12. Regional  $K$ -TSI relationships for Hercynian and Alpine rocks of western Europe.  $\blacktriangle$  Hercynian rocks (hydrofracturing);  $\bullet$  Hercynian rocks (overcoring);  $\blacksquare$  Hercynian rocks (doorstopper);  $\triangle$  Alpine rocks (hydrofracturing);  $\bullet$  Alpine rocks (overcoring) and  $\blacksquare$  Alpine rocks (doorstopper); — regional  $K$ -TSI relationship for western and central European Hercynian rocks; - - regional  $K$ -TSI relationship for western and central European Alpine rocks.

the data show a deviation of  $K \pm 0.5$ , while for the regional  $K$ -TSI relationship (8) and (9) this deviation of  $K \pm 0.5$  was shown by 84% of the data.

The decision tree was used to estimate the magnitude of horizontal stresses in 11 zones of Spain, for which horizontal stress magnitudes and the necessary geological and geophysical data were available.

Using these data (Vera, 2004; Fernández et al., 1998; Tejero and Ruiz, 2002), decision trees 1 and 2 were constructed (see Table 2 and Figs. 3 and 4 for the data used).

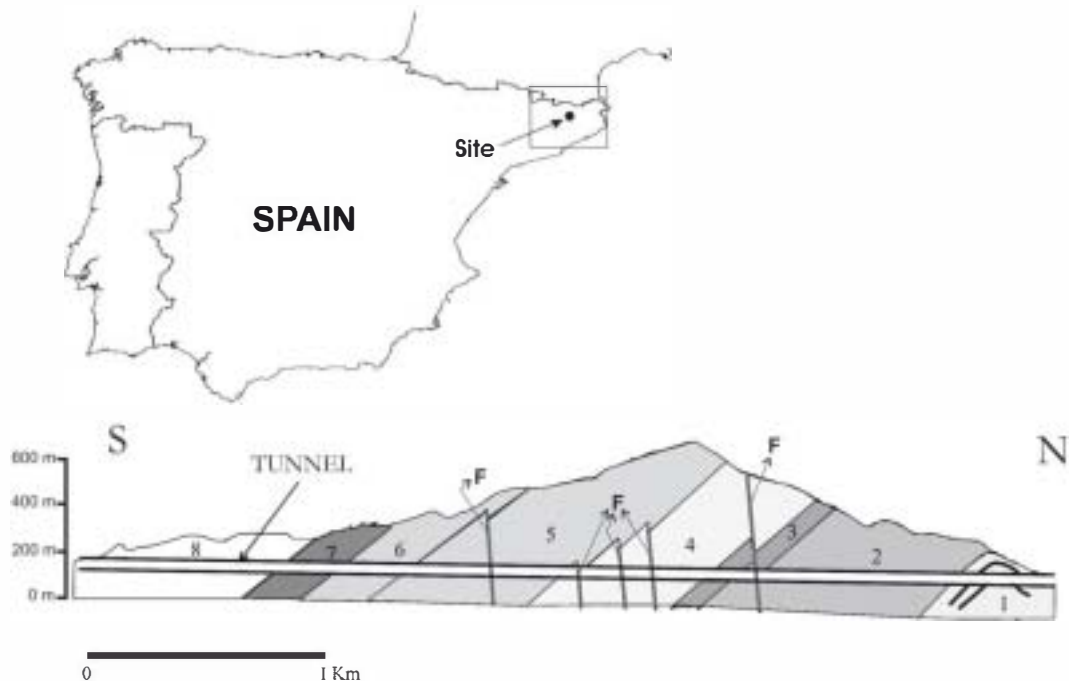
By comparing the in situ determined horizontal stress magnitudes with those estimated by the decision trees, out of 11 cases analysed, for 10 the results of the decision trees were correct and for 9 both the decision tree and TSI results were consistent with in situ  $K$  measurements.

For other central and western European areas, stress magnitude data has been grouped together since these regions show similar stress orientations (Gölke and Coblenz, 1996). These data indicate  $K$  values for Hercynian rocks of 1 to 2 (Fig. 12). The  $K$ -TSI relationship obtained for Hercynian rocks shows a somewhat different relationship to that derived from the world data Eq. (6). In contrast, for Alpine rocks the relationship obtained was close to that based on world data.

## 7. Worked example

As an example of the use of the decision tree and TSI, a case study to determine the stress state of a rock mass for a 4.2 km-road tunnel project in NE Spain was performed (Fig. 13). The materials are sedimentary rocks (shales, sandstones and conglomerates), and the maximum overburden of the tunnel is 550 m. The tunnel's geological location is the southern flank of the great Bellmunt anticline, within the folded foreland of the Pyrenean Range. Crust thickness in this region ranges from 30 to 40 km and heat flow from 50 to 70  $\text{mW m}^{-2}$ . No great relief differences exist in the area, although some faults that could locally modify the state of stress were observed. These data were used to develop decision trees 1 and 2 shown in Figs. 14 and 15. The results obtained indicate that foreseeable horizontal stresses are intermediate ( $10 \text{ MPa} < \sigma_H \leq 25 \text{ MPa}$ ) at a 63% confidence level. Local amplification effects on horizontal stresses would be expected at an 80% level of confidence.

The TSI was calculated using Eq. (1).  $T$  was taken as 12 M.a. given these are Tertiary rocks affected by the Alpine orogen. The value of  $H$



1: Marls, 2: Sandstones, 3: Sandstones and marls, 4: Shales, sandstones and conglomerates, 5: Sandstones and marls, 6: Sandstones, 7: Sandstones and conglomerates, 8: Shales. F: Fault

Fig. 13. Case study location.

was estimated as 1200 to 1500 m from the stratigraphic columns inferred from geological maps of the zone and the tunnel's geological cross-section, although we only considered the top limit of this range. The modulus  $E$  was obtained by uniaxial compressive strength tests using extensimetric bands at 30 GPa. Incorporating these data in Eq. (1) gives a TSI=2.42.  $K$  was calculated from the  $K$ -TSI relationship for Alpine rocks Eq. (7) rendering  $K=1.09$ .

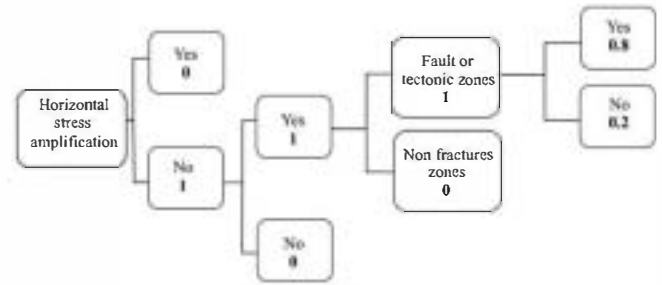
Hydrofracturing tests in the tunnel provided  $K$  values in the range 0.86 to 1.57 for depths of 200 to 440 m, with a representative range of 1-1.5. Thus, the  $K$  value estimated from the TSI was within the mean range obtained in situ and was also consistent with the decision tree results.

### 8. Conclusions

This paper describes a new method of estimating the magnitude of horizontal stresses generated by tectonic activity. The method is based on jointly applying the decision tree probabilistic method and the empirical relationship between the TSI index and in situ determined  $K$  values comprising an extensive database.

The procedure considers the main factors that affect stresses of tectonic origin. In the decision tree, the factors taken into account are geodynamic and geophysical factors that affect the state of stress. The

INFLUENCE FACTORS AT LOCAL SCALE	Topographical effects	Preexistent loads	Tectonized zones present in the area	Stress amplification
----------------------------------	-----------------------	-------------------	--------------------------------------	----------------------



$$\text{Yes} = 0.8 \cdot 1 \cdot 1 \cdot 1 = 0.8 = 80\%$$

$$\text{No} = 0.2 \cdot 1 \cdot 1 \cdot 1 = 0.2$$

Fig. 15. Decision tree 2 for the case study.

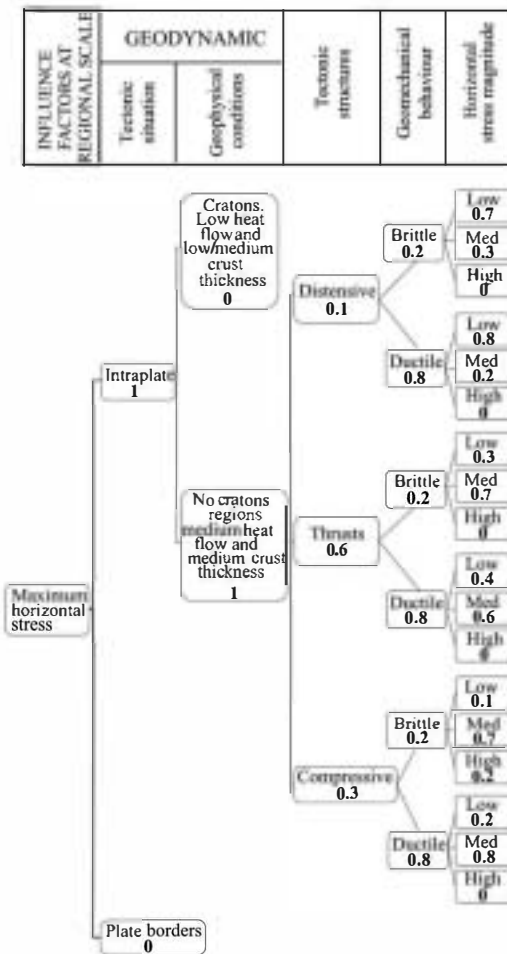
decision tree estimates the magnitudes of horizontal stresses due to regional stress fields grading them as high, intermediate or low. In addition, it determines the likelihood of stress amplification due to local effects. The results are expressed as a probability or degree of confidence. The TSI index takes into account geological and geomechanical factors that may affect stress magnitudes such as the age of the rock deformation, the elastic modulus of the rock or its maximum lithostatic load. From the TSI and its relationship with in situ determined  $K$  values, a value of  $K$  for the rock mass under study is obtained.

13854 data from the WSM, literature reviews and underground projects have been analysed, and selected those showing stress magnitudes of acceptable quality along with the corresponding geological and geomechanical information on the rock mass. This analysis rendered 172 data representing a wide geographical distribution. These data were then used to establish relationships between in situ measured  $K$  values and values of the TSI index, both for data from the same region and for the entire data set.

Several  $K$ -TSI relationships were examined for a regional setting, for Europe and also on a world wide basis using the entire data set. For Spain, 84% of the empirical  $K$  values estimated from the regional  $K$ -TSI relationship showed a variation of  $K \pm 0.5$  with respect to  $K$  values measured in situ, while this variation was exhibited by 72% of the  $K$  values estimated from the  $K$ -TSI'06 global relationship. Similar results were obtained for the remaining regions examined. Moreover,  $K$ -TSI relationships for the global data set (TSI'06 database) revealed a deviation lower or equal to  $K \pm 0.5$  for 63% of the data and one of  $K \pm 0.7$  for 74%. The lowest deviations observed corresponded to  $K$ -TSI relationships within a single region. This is the consequence of the greater uniformity of geological conditions and less uncertainties in calculating the variables comprising the TSI index. In any case, both regional deviations and, in larger measure, global ones, reflect the complexity of the factors contributing to the state of stress and the hypotheses of TSI index, along with the uncertainties inherent in the stress measurements themselves.

By applying the decision tree procedure to 11 Spanish zones, the results for 10 of these zones were consistent with in situ stress measurements and for 9 zones, both the decision tree and the  $K$  values determined empirically based on the TSI index were comparable to instrumental  $K$  measurements.

Through the combined use of the decision tree and TSI index it is possible to estimate the magnitude of major horizontal tectonic stresses in terms of  $K$  values. The use of this procedure will also



$$\text{Low magnitude} = 1 \cdot 1 \cdot (0.7 \cdot 0.2 \cdot 0.1 + 0.8 \cdot 0.8 \cdot 0.1 + 0.3 \cdot 0.2 \cdot 0.6 + 0.4 \cdot 0.8 \cdot 0.6 + 0.1 \cdot 0.2 \cdot 0.3 + 0.2 \cdot 0.8 \cdot 0.3) = 0.36$$

$$\text{Medium magnitude} = 1 \cdot 1 \cdot (0.3 \cdot 0.2 \cdot 0.1 + 0.2 \cdot 0.8 \cdot 0.1 + 0.7 \cdot 0.2 \cdot 0.6 + 0.6 \cdot 0.8 \cdot 0.6 + 0.7 \cdot 0.2 \cdot 0.3 + 0.8 \cdot 0.8 \cdot 0.3) = 0.628 \approx 63\%$$

$$\text{High magnitude} = 1 \cdot 1 \cdot 0.2 \cdot 0.2 \cdot 0.3 = 0.012$$

Fig. 14. Decision tree 1 for the case study.

contribute to interpreting in situ stress measurements and extrapolating them to different zones of the rock mass.

## Acknowledgements

The authors are grateful to Prof. John Hudson from Imperial College of London for his valuable comments and suggestions. Also we thank the suggestions of Prof. C. Li, Trondheim University, Norway; Dr. Y. Shang, Engineering Geomechanics Laboratory, Chinese Academy of Science, Beijing; Dr. Mercedes Ferrer, Geological Survey of Spain IGME; Dr. Juan M. Insúa, Universidad Complutense de Madrid, Dr. Julian Bommer from Imperial College, London and Dr. Julián García-Mayordomo, IGME, Spain. Special thanks to Sr. Angel Rodríguez Soto, In Situ Testing, Madrid who provided hydrofracture test from Spain. We are very gratefully to the reviewer Prof. Ove Stephansson for many helpful comments on our manuscript.

## References

- Amadei, B. and Stephansson, O., 1997. Rock stress and its measurement. Ed. Chapman and Hall.
- Bommer, J., Scherbaum, F., Bungum, H., Cotton, F., Sabetta, F., Abrahamson, N.A., 2005. On the use of logic trees for ground-motion prediction equations in seismic-hazard analysis. *Bulletin of the Seismological Society of America* 95 (2), 377–389.
- Bott, M.H.P., Kuszniir, N.J., 1984. The origin of tectonic stress in the lithosphere. *Tectonophysics* 105, 1–13.
- Buddington, A.F., 1959. Granite emplacement with special reference to North America. *Geological Society of America Bulletin* 70, 671–747.
- Coppersmith, K.J., Young, R.R., 1986. Capturing uncertainty in probabilistic seismic hazard assessments within intraplate environment. *Proceedings of the 3rd National Conference on Earthquake Engineering (Charleston)* South Carolina, 1, pp. 301–312.
- EPRI, 1987. Seismic hazard methodology for the Central and Eastern United States. Seismicity Owners Group and Electric Power Research Institute, P101-38-45-46, 2256-14, Report NP-472.
- Fernández, M., Marzán, I., Correia, A., Ramalho, E., 1998. Heat flow, heat production, and lithospheric thermal regime in the Iberian Peninsula. *Tectonophysics* 291, 29–53.
- Gölke, M., Coblenz, D., 1996. Origins of the European regional stress field. *Tectonophysics* 266, 11–24.
- González de Vallejo, L.I., Serrano, A., Capote, R., De Vicente, G., 1988. The state of stress in Spain and its assessment by empirical methods. *Proc. Int. ISRM Symposium on Rock Mechanics and Power Plants*. Balkema, Madrid, pp. 165–172.
- Goodman, R.E., 1989. *Introduction to Rock Mechanics*, 2nd. Wiley.
- Hijazo, T., 2004. Empirical methods to estimate natural stress of tectonic origin (in Spanish). MSc. Thesis on Engineering Geology. Universidad Complutense de Madrid.
- Hoek, E., Brown, E.T., 1980. *Underground Excavations in Rock*. Inst. of Mining and Metallurgy, London.
- ISRM, 2003. Special issue of the IJRMMS: rock stress estimation ISRM suggested methods and associated supporting papers. *Int. J. Rock. Mech. Min. Sci. Geomech.* 40 (7–8), 955–1276.
- Kuszniir, N.J., 1991. The distribution of stress with depth in the lithosphere: thermo-rheological and geodynamic constraints. *Phil. Trans. R. Soc. Lond. A* 337, 95–110.
- Kuszniir, N.J., Bott, M.H.P., 1977. Stress concentration in the upper lithosphere caused by underlying visco-elastic creep. *Tectonophysics* 43, 247–256.
- Lin, W., Hirono, T., Nakamura, T., Yamamoto, K., Matsui, K., Imamura, T., Oikawa, Y., Takahashi, M., Kwasniewski, M., 2003. Determination of rock stress by anelastic strain recovery measurement of an oriented core in the Nittsu region of Japan. *Proceedings of the 3th International Symposium on Rock Stress RS Kumamoto, Balkema, Kumamoto (Japan)*, pp. 225–229.
- Olaiz, A., De Vicente, G., Muñoz-Martín, A., Vegas, R., 2006. Mapa de esfuerzos de Europa a partir de mecanismos focales calculados desde el tensor momento sísmico. *Geogaceta* 40, 55–58.
- Park, R.G., 1988. *Geological structures and moving plates*. Ed. Blackie and Son.
- Reinecker, J., Heibach, O., Tingay, M., Connolly, P. and Müller, B., 2004. The 2004 release of the World Stress Map (available online at [www.world-stress-map.org](http://www.world-stress-map.org)).
- Reiter, L., 1990. *Earthquake Hazard Analysis. Issues and Insights*. Columbia University Press, New York.
- Sheorey, P.R., 1994. A theory of in-situ stress in isotropic and transversely isotropic rock. *Int. J. Rock. Mech. Min. Sci. Geomech.* 31 (1), 23–34.
- Tejero, R., Ruiz, J., 2002. Thermal and mechanical structure of the central Iberian Peninsula lithosphere. *Tectonophysics* 350, 49–62.
- US Army Corps of Engineers Internet Publishing Group, 1999. Engineer Manuals "Response Spectra and Seismic Analysis for Concrete Hydraulic Structures". [www.usace.army.mil/inet/usace-docs/eng-manuals/em.htm](http://www.usace.army.mil/inet/usace-docs/eng-manuals/em.htm).
- Vera, J.A. (Ed.), 2004. *Geología de España*. SGE-IGME, Madrid. 890 p.
- Villaescusa, E., Seto, M., Baire, G., 2002. Stress measurements from oriented core. *Int. J. Rock. Mech. Min. Sci. Geomech.* 39 (5), 603–615.
- Zoback, M.L., et al., 1989. Global patterns of tectonic stress. *Nature* 341, 291–298.